HHS Public Access

Author manuscript

J Biomech. Author manuscript; available in PMC 2017 September 06.

Published in final edited form as:

J Biomech. 2016 September 6; 49(13): 2756–2762. doi:10.1016/j.jbiomech.2016.06.008.

Region and Strain-dependent Diffusivities of Glucose and Lactate in Healthy Human Cartilage Endplate

Yongren Wu[1,2], **Sarah E. Cisewski**[1], **Nicholas Wegner**[1], **Shichang Zhao**[1], **Vincent D. Pellegrini Jr**[2], **Elizabeth H. Slate**[3], and **Hai Yao**[1,2]

[1]Department of Bioengineering, Clemson University, Clemson, SC

[2]Department of Orthopaedics, Medical University of South Carolina (MUSC), Charleston, SC

[3]Department of Statistics, Florida State University, Tallahassee, FL

Abstract

The cartilage endplate (CEP) is implicated as the main pathway of nutrient supply to the healthy human intervertebral disc (IVD). In this study, the diffusivities of nutrient/metabolite solutes in healthy CEP were assessed, and further correlated with tissue biochemical composition and structure. The CEPs from non-degenerated human IVD were divided into four regions: central, lateral, anterior, and posterior. The diffusivities of glucose and lactate were measured with a custom diffusion cell apparatus under 0%, 10%, and 20% compressive strains. Biochemical assays were conducted to quantify the water and glycosaminoglycan (GAG) contents. The Safranin-O and Ehrlich's hematoxylin and eosin staining and scanning electron microscopy (SEM) were performed to reveal the tissue structure of the CEP. Average diffusivities of glucose and lactate in healthy CEP were $2.68\pm0.93\times10^{-7}$ cm^2/s and $4.52\pm1.47\times10^{-7}$ cm^2/s, respectively. Solute diffusivities were region-dependent ($p<0.0001$) with the highest values in the central region, and mechanical strains impeded solute diffusion in the CEP ($p<0.0001$). The solute diffusivities were significantly correlated with the tissue porosities (glucose: $p<0.0001$, $r=0.581$; lactate: $p<0.0001$, $r=0.534$). Histological and SEM studies further revealed that the collagen fibers in healthy CEP are more compacted than those in the nucleus pulposus (NP) and annulus fibrosus (AF) and show no clear orientation. Compared to human AF and NP, much smaller solute diffusivities in human CEP suggested that it acts as a gateway for solute diffusion through the disc, maintaining the balance of nutritional environment in healthy human disc under mechanical loading and preventing the progression of disc degeneration.

Address for Correspondence: Hai Yao, PhD, Department of Bioengineering, Clemson University, CU-MUSC Bioengineering Program, 173 Ashley Avenue, MSC 508, Charleston, SC 29425, Phone: (843)876-2380, Fax: (843)792-6626, haiyao@clemson.edu.

CONFLICT OF INTEREST STATEMENT

None of the authors of this paper have a conflict of interest that might be construed as affecting the conduct or reporting of the work presented.

Keywords

Intervertebral disc; Nutrient transport; Cartilage endplate; Solute diffusivity; Mechanical strain

INTRODUCTION

The cartilage endplate (CEP), a thin layer of hyaline cartilage at the cranial and caudal surfaces of human intervertebral disc (IVD), was found to be the main pathway of nutrient supply to the disc through *in vivo* and *in vitro* studies (Maroudas, et al., 1975; Nachemson, et al., 1970; Ogata and Whiteside, 1981; Urban, et al., 1982). Due to the avascular nature of the disc, the nutrients from the capillaries in the subchondral plates diffuse into the disc through the CEPs, while the metabolites diffuse out through a reversed direction (Huang, et al., 2014). Pathological change, such as CEP calcification at the early stage of disc degeneration, could break down the precautious nutritional balance inside the disc by impeding nutrient/metabolite diffusion through the disc (Benneker, et al., 2005; Roberts, et al., 1993). By contrast, fractured or degenerated CEPs have been found to co-occur in severely degenerated discs (Adams and Hutton, 1982; Veres, et al., 2010). The lesions in the CEP can open up channels and hasten the inflow of cytokines, enzymes or angiogenic molecules which have deleterious effects on disc cells and further accelerate disc degeneration (Koike, et al., 2003; Rajasekaran, et al., 2004; Roberts, et al., 1996). The differential effects of the CEP on solute transport through the disc at different degeneration stages suggested that healthy CEP is a critical disc component for maintaining the unique disc nutritional environment under the physiological condition. The collapse of the balance between nutrient supply and intrinsic cellular demand inside the disc is considered one of the major factors for disc degeneration (Huang, et al., 2014; Roberts, et al., 1993).

The CEP has unique biomechanical properties from other disc components [annulus fibrosus (AF) and nucleus proposes (NP)] and articular cartilage (Wu, et al., 2015). Although the solute diffusion behaviors in human CEP were previously studied using the fluorescein-labeled markers and contrast agents (Rajasekaran, et al., 2004; Rajasekaran, et al., 2010; Roberts, et al., 1996), the diffusivity values of basic nutrient/metabolite (i.e., glucose/lactate) in healthy or degenerated human CEP are largely unknown. Glycolysis is believed to be the major energy metabolism pathway for disc cells *in vivo* by consuming glucose to generate adenosine triphosphate (ATP) and producing lactic acid as a waste product (Bibby, et al., 2005). Therefore, the knowledge about the diffusion rates of glucose and lactate in human CEP is crucial for understanding disc nutrition.

The rate of solute diffusion in cartilaginous tissue is governed by solute diffusivities which are affected by the composition and structure of the tissue matrix, as well as mechanical strains on the tissue (Jackson and Gu, 2009). Therefore, the objective of this study was to measure the nutrient/metabolite diffusivities of healthy human CEPs in four regions (central, lateral, anterior, and posterior) under three compressive strains (0%, 10%, and 20%). Specifically, the effect of mechanical strain on the glucose/lactate diffusivities in the CEP was determined using the diffusion cell method (Jackson, et al., 2008). Biochemical compositions of the CEP were characterized and correlated with the diffusion properties.

The microstructures of healthy human CEP were further revealed using histological staining techniques and scanning electron microscopy (SEM). We hypothesized that the diffusivities of glucose and lactate in healthy human CEP were region-dependent due to its unique tissue composition and structure; and mechanical loading impacts the rates of solute diffusion in this tissue by changing the tissue hydration. The goal of this study was to establish a baseline measurement of nutrient/metabolites diffusivities in healthy human CEPs. The results of this study may facilitate the understanding of the role of human CEP in IVD nutrition and provide new insights into nutrition-related mechanisms of disc degeneration and regeneration.

METHODS

Specimen Preparation

Twelve human lumbar spines (33–65 years old) obtained from an Organ Procurement Organization (LifePoint Inc., Charleston, SC) were screened based on the Thompson grading system (Thompson, et al., 1990) under an institutional approval. To establish a quality baseline measurement in healthy CEPs, only spines without degenerated discs (Grade III–V) and related diseases were selected. To limit the tissue variation, only L2–L3 and L3–L4 discs were used. Further, only healthy CEPs without artifacts, such as fissures and calcification, were included for the measurements. Considering these criteria, six disc motion segments were harvested from three lumbar spines within 24 hours after death (58 year old female, 42 year old male, and 54 year old female). Three L3–L4 disc motion segments were used for diffusion experiments, while three L2–L3 disc motion segments were used for histological and SEM studies. Healthy human CEPs were harvested and tested within three days after receiving the spine.

The disc motion segments were opened through the median plane of the disc with a scalpel. Cylindrical plugs of NP or AF/endplate/bone were extracted from four regions (center, lateral, anterior, and posterior) from both superior and inferior surfaces of the disc with an 8 mm diameter corneal trephine (Figure 1). The plugs harvested from the left lateral region were used for diffusion, histological staining and SEM protocol development. The right lateral region was used for diffusivity and image data collection. The plug was microtomed to carefully remove the overlying NP/AF (relatively more transparent than CEP tissue) and the vertebral bone. The final disc-shape CEP specimens were punched out with a 6 mm diameter trephine for the diffusion experiment. The specimen preparation was conducted in a moisturized hood to prevent tissue dehydration. The prepared CEP specimens (n=24, from 3 L3–4 discs of 3 spines) had an average initial thickness of 0.734±0.103 mm, which is in the same range as stated in previous studies (Roberts, et al., 1989).

Glucose and Lactate Diffusivity Measurements

A previously established custom diffusion cell was used to measure the strain-dependent diffusivities of glucose and lactate in the CEP specimens (Jackson, et al., 2012; Jackson, et al., 2008). It consisted of two non-conductive acrylic solution chambers with a channel separated by the specimen holder (Figure 1B). The specimen was held between two rigid porous plates (hydrophilic polyethylene, 50–90 μm pore size, Small Parts, Inc., Miami

Lakes, FL) to inhibit swelling and sealed with an O-ring. The compressive strains were applied to the CEP specimens by changing of the spacers placed between the two chamber halves.

The CEP specimen was first held at its initial thickness (0% strain level). 500 μL of 20 mg/mL glucose with 10 mg/mL lactate mixed into normal phosphate-buffered saline (PBS) was pipetted into the upstream chamber while 200 μL of concentrated PBS solution was pipetted into the downstream chamber. The concentrated PBS solution was used to balance the osmolarity of the glucose/lactate solution in the upstream chamber (530 mOsm/L) to prevent any convection through the specimen due to osmosis. The diffusion cell was placed in an incubator with 37°C. The stir bars were utilized to maintain constant solute distribution within the solution. After glucose and lactate were allowed to diffuse through the tissue specimen for a 15-minute time interval, the contents of the downstream chamber were emptied and glucose and lactate concentrations were measured with YSI 2700 Select Biochemistry Analyzer (YSI Inc., Yellow Springs, OH). Following each 15-minute time interval, the downstream chamber was refilled with 200 μL of fresh PBS solution, while the upstream chamber was refilled with 500 μL of fresh glucose/lactate solution. The experiment was repeated until the same concentration (within 5%) in the downstream chamber was obtained for 2–3 consecutive readings, suggesting that steady state had been reached. An average of 2.5 hours (10 intervals of 15 minutes each) was necessary to reach steady state. Once steady state was achieved at 0% compression, the experiment was repeated for 10% and 20% compressive strains. The apparent diffusivity (D_{app}) was calculated based on the one-dimensional steady state diffusion theory (Jackson, et al., 2008):

$$D_{app}=ln\frac{C_{up}-C_{down}(t_0)}{C_{up}-C_{down}(t)}\frac{V_{down}h}{A(t-t_0)} \quad (1)$$

where C_{up} is the concentration in the upstream chamber which is assumed to be constant. $C_{down}(t_0)$ is the downstream concentration at initial diffusion time t_0 and $C_{down}(t)$ is the concentration at time t. h is the thickness of the specimen, and A is the cross section area through which the diffusive flux occurs. This area was calculated as 50% of the area of the porous plates confining the specimen, as the porous material has a 50% open area. V_{down} is the volume in the downstream well. Due to solution replacement at the start of each 15-minute interval, the value of $C_{down}(t_0)C_{down}(t)$ is the averaged value of the 2–3 consecutive readings of downstream concentration at steady state.

Histological and SEM Studies

Bone/CEP/disc tissue plugs were taken at the four regions from both superior and inferior surfaces of two disc motion segments at L2–L3 level (Figure 1A). The plugs were rapidly fixed in 10% neutral buffered formalin, decalcified, and paraffin wax embedded. Ehrlich's hematoxylin and eosin (H&E) and Safranin-O & Fast Green were used with the wax sections (7 μm). For the SEM study, bone/CEP/disc tissue plugs were taken from one disc motion segment at L2–L3 level. The plugs from the inferior surface were microtomed to remove both bone and disc tissue to reveal the collagen fibers of the CEP on the horizontal

plane (X–Y plane; Figure 2). Meanwhile, the plugs from superior surface were cut anteroposteriorly to show the microstructures of bone, CEP, and disc tissue on the vertical plane (Y–Z plane; Figure 2). The specimens were then fixed in PBS solution with 2.5% glutaraldehyde, dehydrated with a series of ethanol, and dried in hexamethyldisilazane (HMDS) solution. A gold layer with 20 nm thickness was coated on the specimens to enhance contrast. Images were taken under a JEOL JSM-5600LV SEM (JEOL USA, Inc., Pleasanton, CA) at 35x, 50x, and 500x magnifications.

Porosity and GAG Measurements

A buoyancy method was used to determine the initial porosity (ratio of water volume to wet tissue volume) of the CEP specimens at 0% strain level (Gu, et al., 1996):

$$\Phi_0^w = \frac{W_{wet} - W_{dry}}{W_{wet} - W_{PBS}} \frac{\rho_{PBS}}{\rho_w} \quad (2)$$

where Φ_0^w is initial porosity, W_{wet}, W_{PBS}, and W_{dry} are weights of specimens in the air, in PBS solution and after lyophilized. ρ_{PBS} and ρ_w are the densities of the PBS solution and water. The porosities of the CEPs under 10% and 20% strain levels were calculated based on the relationship between tissue porosity and dilatation e (e = J−1 where J is the tissue deformation) (Lai, et al., 1991),

$$\Phi^w = \frac{\Phi_0^w + e}{1 + e} \quad (3)$$

The lyophilized tissues were then assayed for glycosaminoglycan (GAG) content. The Blyscan Glycosaminoglycan Assay kit (Biocolor Ltd., Newtonabbey, Northern Ireland) was used to determine the GAG content based on 1,9-dimethylmethylene blue dye binding, with standards provided by the manufacturer.

Statistical Analysis

The measurements were reported using the means and standard deviations (SD). The glucose and lactate diffusivities were examined for significant differences by mechanical strain and disc region using two-way ANOVA that allowed for correlation among measurements from the same spine and also incorporated error heterogeneity by disc region. The porosity and GAG content were similarly examined for differences by disc region. Correlations between solute diffusivities and porosity were determined marginally (Nakagawa and Schielzeth, 2013) using the linear mixed effects model with a random effect for spine. Due to the limited sample size, the sex and age effects were not considered in this study. The statistical analysis was conducted in R (R Core Team, 2015) using the package nlme.

RESULTS

Glucose and Lactate Diffusivities

The apparent glucose and lactate diffusivities were measured for healthy human CEP at 0%, 10%, and 20% compressive strains (Figure 3A&B). A significant strain effect was found for the diffusivities of both solutes ($p<0.0001$). The cross-region glucose diffusivity at 0% strain was $2.68\pm0.93\times10^{-7}$ cm^2/sec, at 10% strain it decreased to $1.96\pm0.81\times10^{-7}$ cm^2/sec (−27%), and at 20% strain was $1.44\pm0.68\times10^{-7}$ cm^2/sec (−46%). The lactate diffusivity was $4.52\pm1.47\times10^{-7}$ cm^2/sec, $3.56\pm1.20\times10^{-7}$ cm^2/sec (−21%) and $2.76\pm1.08\times10^{-7}$ cm^2/sec (−39%) for 0%, 10%, and 20% strains, respectively. A significant regional effect was also found for the diffusivities of both solutes ($p<0.0001$). The glucose diffusivity in the central region at 0% strain (Central: $3.44\pm0.97\times10^{-7}$ cm^2/sec) was significantly higher than in the lateral and posterior regions (Lateral: $2.46\pm0.86\times10^{-7}$ cm^2/sec, $p=0.020$; Posterior: $1.91\pm0.39\times10^{-7}$ cm^2/sec, $p<0.0001$). The lactate diffusivity in the central region at 0% strain (Central: $5.52\pm1.52\times10^{-7}$ cm^2/sec) was also significantly higher than in the lateral and posterior regions (Lateral: $4.11\pm1.48\times10^{-7}$ cm^2/sec, $p=0.036$; Posterior: $3.36\pm0.64\times10^{-7}$ cm^2/sec, $p<0.0001$). No significant difference was detected for both glucose and lactate diffusivities between central and anterior regions (Glucose: $2.78\pm0.83\times10^{-7}$ cm^2/sec, $p=0.085$; Lactate: $4.88\pm1.34\times10^{-7}$ cm^2/sec, $p=0.391$). There was no evidence for an interaction between region and strain for either glucose ($p=0.983$) or lactate ($p=0.986$).

Porosity and GAG content

The cross-region porosity in CEP was 0.667 ± 0.049 (at 0% mechanical strain) and significant variation among the four regions was detected ($p=0.034$) with the central region having higher values ($p<0.04$) than the anterior and posterior regions, but not differing from the lateral region ($p=0.31$) (Table 1). The average GAG content in CEP was 90.08 ± 17.77 μg/mg dry tissue and also differed among the four regions ($p=0.001$) with the central region significantly higher than the lateral, anterior, and posterior regions ($p<0.009$).

Histological Appearance and Collagen Fiber Microstructure

Histological images (H&E; Safranin-O&Fast Green) showed that there was a thin layer of cartilage endplate between the interface of the human vertebral body and disc tissue (Figure 2A). In the Safranin-O images, the CEP region appeared to be bright red. The thickness of the CEP varied by region, with a value between 0.6 mm and 1.2 mm. SEM images further revealed the unique sandwich structure consisted of bone, CEP, and disc tissue (Figure 2B). It is apparent that collagen fibers in CEP layer were more compacted compared to NP and AF tissues. There is no clear fiber orientation in both horizontal and vertical planes for the CEP.

Correlation between Material Properties and Tissue Biochemical Composition

The correlations between solute diffusivities (glucose and lactate) and porosities were found to be statistically significant, as shown in Figure 4A&B (Glucose: $r=0.581$, $p<0.0001$, $n=72$; Lactate: $r=0.534$, $p<0.0001$, $n=72$). No statistical significant correlations were observed between solute diffusivities and GAG contents ($p>0.11$).

DISCUSSION

This study was commenced to determine the baseline nutrient/metabolite solute (glucose and lactate) diffusivities in healthy human CEP and further investigate the effects of disc region and mechanical strain on the tissue transport properties. The results showed that the solute diffusivities in human CEP were much smaller than those in other disc components (e.g., AF) and articular cartilage (Table 2). This suggested that healthy human CEP may act as a gateway for nutrient/metabolite solute inflow/outflow through the disc (Nachemson, et al., 1970; Roberts, et al., 1996). The mechanical strain-dependent solute diffusivities further suggested that CEP may facilitate the maintenance of a stable extracellular nutrient environment by impeding the solute transport through the disc under mechanical loading conditions. These results correspond to recent findings in the literature that the CEP could act as a mechanical barrier by facilitating interstitial fluid pressurization and resisting disc herniation under abnormal loadings (Fields, et al., 2014; Rajasekaran, et al., 2013; Wu, et al., 2015). In addition, the results of this study further supported the previous notion that healthy CEP may play an important role in ECM homeostasis and the progression of angiogenesis, which is associated with disc degeneration, by blocking the rapid diffusion of cytokines, enzymes, or angiogenic molecules such as vascular endothelial growth factor (VEGF) into the disc (Koike, et al., 2003; Lotz and Ulrich, 2006; Rajasekaran, et al., 2004; Roberts, et al., 1996; Urban and McMullin, 1988).

Conversely, due to the avascular nature of human IVD, the main pathway for nutrient supply to the disc is diffusion through the CEP. The low solute diffusivities in the CEP can lead to a critical nutrient environment in human IVD (i.e., a steeper nutrient/metabolite gradient with low oxygen and glucose, and high lactate concentrations at the center of the disc) (Urban, et al., 1982). Such delicate nutrient environment may be vulnerable to any pathological changes of the CEP, such as calcification (Huang, et al., 2014; Roberts, et al., 1996). The deterioration of the extracellular nutrient environment will change the metabolism and synthesis behaviors of disc cells and affect the cell viability, leading to initiate/accelerate disc degeneration (Bibby, et al., 2005; Bibby and Urban, 2004; Guehring, et al., 2009; Ishihara and Urban, 1999).

The diffusivities of nutrient/metabolite solutes were found to be region-dependent with significantly higher values in the central region, which is consistent with a previous study of glucose diffusivities in human CEP (Maroudas, et al., 1975). This can be associated with the regionally dependent biochemical composition in the CEP with the highest porosity being in the central region. Our results showed that the glucose and lactate diffusivities in healthy human CEP were significantly correlated with the tissue porosities instead of the GAG contents. This finding further supported the previous hypothesis that water content is generally a dominated determinant for the diffusion properties of small solutes (molecular weight < 5000 Dalton) in cartilaginous tissues (Gu, et al., 2004; Nimer, et al., 2003; Torzilli, et al., 1997). Compared to other disc components and articular cartilage, the smaller solute diffusivities in healthy human CEP can also be attributed to its ECM structure with compacted collagen fibers, as shown in our histological and SEM studies (Figure 2). This was in agreement with the high collagen content and tensile modulus of human CEP in a recent study (Fields, et al., 2014).

Due to the technical challenges of *in vivo* measurements, finite element (FE) models were commonly used to predict the extracellular mechano-electrochemical environment in the human IVD (Huang and Gu, 2008; Jackson, et al., 2011; Shirazi-Adl, et al., 2010; Soukane, et al., 2007). Although there were a variety of characterizations on material properties of AF and NP tissues (Gu, et al., 1999; Maroudas, et al., 1975; Nachemson, et al., 1970; Roberts, et al., 1996; Setton, et al., 1993), the tissue properties, especially transport properties, of human CEP are rare. Consequently, the CEP were either excluded or modeled with material properties of other disc components or articular cartilage in current FE models. Our results clearly showed that the diffusion properties of human CEP were significantly different from other disc components (Table 2). Therefore, the region and strain-dependent solute diffusivities, as well as the porosities, determined in this study should be incorporated into the FE models to better predict the physiological nutrient environment in human IVD, which can serve as a baseline for future analysis on disc degeneration and regeneration.

Several limitations of this study should be noted. To establish a quality baseline measurement in healthy human CEP, the disc motion segments were screened by age (30–65 years old), disc level (L2–L4), and degeneration conditions (Grade I–II). Although only twenty four healthy CEP specimens obtained from three fresh, healthy, and mature lumbar spines were eligible for the diffusion study, the results successfully demonstrated the statistical significance for testing the hypothesis. Due to the scarcity of human disc samples, a future study with a larger sample size needs to be conducted to fully understand how other factors (e.g. age, sex, disc level, and CEP calcification) affect the diffusion properties in the CEP and gain a further understanding on the role of CEP in the progression of disc degeneration.

The rigid porous plates in the diffusion cell to compress the specimens may cause a stagnant layer formation between the tissue and the solution, although they were much more permeable than the CEP tissue. The stirring rod could minimize the effect of boundary layer formation, but it may not be eliminated entirely (Maroudas and Bullough, 1968). As shown in the previous studies, a 7% less of the apparent glucose diffusivity was found in porcine articular cartilage which was measured with porous plate than that without porous plate (Jackson, et al., 2012; Jackson, et al., 2008). However, the porous plates were necessary in this study to confine the CEP specimens due to significant tissue swelling and provide the means to control the strain levels of the specimens. In addition, the apparent diffusivities (D_{app}) measured in this study represent the coupling effect of the intrinsic diffusivity (D) and partition coefficient (K) ($D_{app}=KD$). A previous study has shown that the partition coefficient was dependent on the mechanical compression in cartilage tissues (Quinn, et al., 2001). To characterize the intrinsic diffusivity which is more essential for the FE modeling of the IVD, further experiments are necessary to determine the strain-dependent solute partition coefficients in the CEP.

In summary, this study measured the baseline nutrient/metabolite solute (glucose and lactate) diffusivities in healthy human CEP and further studied the effects of disc region and mechanical strain on the tissue transport properties. The diffusivities of glucose and lactate in healthy human CEP were region-dependent due to its unique tissue composition and structure; and mechanical loading impedes the rates of solute diffusion by changing the

tissue porosity. Compared to the AF and NP, human CEP has much smaller solute diffusivities and acts as a gateway for solute diffusion through the disc. The results of this study may facilitate the understanding of the role of human CEP in IVD nutrition and provide new insights into nutrition-related mechanisms of disc degeneration and regeneration.

Acknowledgments

This project was supported by NIH grants AR055775, DE018741 and DE021134, and a NIH T32 predoctoral fellowship DE017551 and a NSF Graduate Research Fellowship to SEC. The authors thank Dr. Steve L. Morton for his valuable assistance in SEM imaging and Dr. Simona Baicu at the LifePoint, Inc. for assisting human spine harvest.

References

Adams MA, Hutton WC. Prolapsed intervertebral disc. A hyperflexion injury. Spine. 1982; 7:184–191. [PubMed: 7112236]

Benneker LM, Heini PF, Alini M, et al. Vertebral endplate marrow contact channel occlusions and intervertebral disc degeneration. Spine. 2005; 30:167–173. [PubMed: 15644751]

Bibby SR, Jones DA, Ripley RM, Urban JP. Metabolism of the intervertebral disc: effects of low levels of oxygen, glucose, and pH on rates of energy metabolism of bovine nucleus pulposus cells. Spine. 2005; 30:487–496. [PubMed: 15738779]

Bibby SR, Urban JP. Effect of nutrient deprivation on the viability of intervertebral disc cells. Eur Spine J. 2004; 13:695–701. [PubMed: 15048560]

Fields AJ, Rodriguez D, Gary KN, et al. Influence of biochemical composition on endplate cartilage tensile properties in the human lumbar spine. J Orthop Res. 2014; 32:245–252. [PubMed: 24273192]

Gu W, Lewis B, Lai WM, Ratcliffe A. A Technique for Measuring Volume and True Density of the Solid Matrix of Cartilaginous Tissues. Advances in Bioengineering, ASME BED. 1996:89–90.

Gu WY, Mao XG, Rawlins BA, et al. Streaming potential of human lumbar anulus fibrosus is anisotropic and affected by disc degeneration. J Biomech. 1999; 32:1177–1182. [PubMed: 10541067]

Gu WY, Yao H, Vega AL, Flagler D. Diffusivity of ions in agarose gels and intervertebral disc: effect of porosity. Ann Biomed Eng. 2004; 32:1710–1717. [PubMed: 15675682]

Guehring T, Wilde G, Sumner M, et al. Notochordal intervertebral disc cells: sensitivity to nutrient deprivation. Arthritis Rheum. 2009; 60:1026–1034. [PubMed: 19333932]

Huang CY, Gu WY. Effects of mechanical compression on metabolism and distribution of oxygen and lactate in intervertebral disc. J Biomech. 2008; 41:1184–1196. [PubMed: 18374341]

Huang YC, Urban JP, Luk KD. Intervertebral disc regeneration: do nutrients lead the way? Nat Rev Rheumatol. 2014; 10:561–566. [PubMed: 24914695]

Ishihara H, Urban JP. Effects of low oxygen concentrations and metabolic inhibitors on proteoglycan and protein synthesis rates in the intervertebral disc. J Orthop Res. 1999; 17:829–835. [PubMed: 10632449]

Jackson A, Gu W. Transport Properties of Cartilaginous Tissues. Curr Rheumatol Rev. 2009; 5:40. [PubMed: 20126303]

Jackson AR, Huang CY, Gu WY. Effect of endplate calcification and mechanical deformation on the distribution of glucose in intervertebral disc: a 3D finite element study. Comput Methods Biomech Biomed Engin. 2011; 14:195–204. [PubMed: 21337225]

Jackson AR, Yuan TY, Huang CY, et al. Nutrient transport in human annulus fibrosus is affected by compressive strain and anisotropy. Ann Biomed Eng. 2012; 40:2551–2558. [PubMed: 22669503]

Jackson AR, Yuan TY, Huang CY, et al. Effect of compression and anisotropy on the diffusion of glucose in annulus fibrosus. Spine. 2008; 33:1–7. [PubMed: 18165741]

Koike Y, Uzuki M, Kokubun S, Sawai T. Angiogenesis and inflammatory cell infiltration in lumbar disc herniation. Spine. 2003; 28:1928–1933. [PubMed: 12973136]

Lai WM, Hou JS, Mow VC. A triphasic theory for the swelling and deformation behaviors of articular cartilage. J Biomech Eng. 1991; 113:245–258. [PubMed: 1921350]

Lotz JC, Ulrich JA. Innervation, inflammation, and hypermobility may characterize pathologic disc degeneration: review of animal model data. J Bone Joint Surg Am. 2006; 88(Suppl 2):76–82.

Maroudas A. Distribution and diffusion of solutes in articular cartilage. Biophys J. 1970; 10:365–379. [PubMed: 4245322]

Maroudas A, Bullough P. Permeability of articular cartilage. Nature. 1968; 219:1260–1261. [PubMed: 5677422]

Maroudas A, Stockwell RA, Nachemson A, Urban J. Factors involved in the nutrition of the human lumbar intervertebral disc: cellularity and diffusion of glucose in vitro. J Anat. 1975; 120:113–130. [PubMed: 1184452]

Nachemson A, Lewin T, Maroudas A, Freeman MA. In vitro diffusion of dye through the end-plates and the annulus fibrosus of human lumbar inter-vertebral discs. Acta Orthop Scand. 1970; 41:589–607. [PubMed: 5516549]

Nakagawa S, Schielzeth H. A general and simple method for obtaining R^2 from Generalized Linear Mixed-effects Models. Methods Ecol Evol. 2013; 4:133–142.

Nimer E, Schneiderman R, Maroudas A. Diffusion and partition of solutes in cartilage under static load. Biophys Chem. 2003; 106:125–146. [PubMed: 14556902]

Ogata K, Whiteside LA. Nutritional pathways of the intervertebral disc. An experimental study using hydrogen washout technique. Spine. 1981; 6:211–216. [PubMed: 7268543]

Quinn TM, Morel V, Meister JJ. Static compression of articular cartilage can reduce solute diffusivity and partitioning: implications for the chondrocyte biological response. J Biomech. 2001; 34:1463–1469. [PubMed: 11672721]

Rajasekaran S, Babu JN, Arun R, et al. A study of diffusion in human lumbar discs: a serial magnetic resonance imaging study documenting the influence of the endplate on diffusion in normal and degenerate discs. Spine. 2004; 29:2654–2667. [PubMed: 15564914]

Rajasekaran S, Bajaj N, Tubaki V, et al. The anatomy of failure in lumbar disc herniation: an in vivo, multimodal, prospective study of 181 subjects. Spine. 2013; 38:1491–1500. [PubMed: 23680832]

Rajasekaran S, Vidyadhara S, Subbiah M, et al. A study of effects of in vivo mechanical forces on human lumbar discs with scoliotic disc as a biological model: results from serial postcontrast diffusion studies, histopathology and biochemical analysis of twenty-one human lumbar scoliotic discs. Spine. 2010; 35:1930–1943. [PubMed: 20838264]

Roberts S, Menage J, Eisenstein SM. The cartilage end-plate and intervertebral disc in scoliosis: calcification and other sequelae. J Orthop Res. 1993; 11:747–757. [PubMed: 8410475]

Roberts S, Menage J, Urban JP. Biochemical and structural properties of the cartilage end-plate and its relation to the intervertebral disc. Spine. 1989; 14:166–174. [PubMed: 2922637]

Roberts S, Urban JP, Evans H, Eisenstein SM. Transport properties of the human cartilage endplate in relation to its composition and calcification. Spine. 1996; 21:415–420. [PubMed: 8658243]

Setton LA, Zhu W, Weidenbaum M, et al. Compressive properties of the cartilaginous end-plate of the baboon lumbar spine. J Orthop Res. 1993; 11:228–239. [PubMed: 8483035]

Shirazi-Adl A, Taheri M, Urban JP. Analysis of cell viability in intervertebral disc: Effect of endplate permeability on cell population. J Biomech. 2010; 43:1330–1336. [PubMed: 20167323]

Soukane DM, Shirazi-Adl A, Urban JP. Computation of coupled diffusion of oxygen, glucose and lactic acid in an intervertebral disc. J Biomech. 2007; 40:2645–2654. [PubMed: 17336990]

Thompson JP, Pearce RH, Schechter MT, et al. Preliminary evaluation of a scheme for grading the gross morphology of the human intervertebral disc. Spine. 1990; 15:411–415. [PubMed: 2363069]

Torzilli PA, Arduino JM, Gregory JD, Bansal M. Effect of proteoglycan removal on solute mobility in articular cartilage. J Biomech. 1997; 30:895–902. [PubMed: 9302612]

Urban JP, Holm S, Maroudas A, Nachemson A. Nutrition of the intervertebral disc: effect of fluid flow on solute transport. Clin Orthop Relat Res. 1982:296–302.

Urban JP, McMullin JF. Swelling pressure of the lumbar intervertebral discs: influence of age, spinal level, composition, and degeneration. Spine. 1988; 13:179–187. [PubMed: 3406838]

Veres SP, Robertson PA, Broom ND. How loading rate influences disc failure mechanics: a microstructural assessment of internal disruption. Spine. 2010; 35:1897–1908. [PubMed: 20838275]

Wu Y, Cisewski SE, Sachs BL, et al. The region-dependent biomechanical and biochemical properties of bovine cartilaginous endplate. J Biomech. 2015; 48:3185–3191. [PubMed: 26209084]

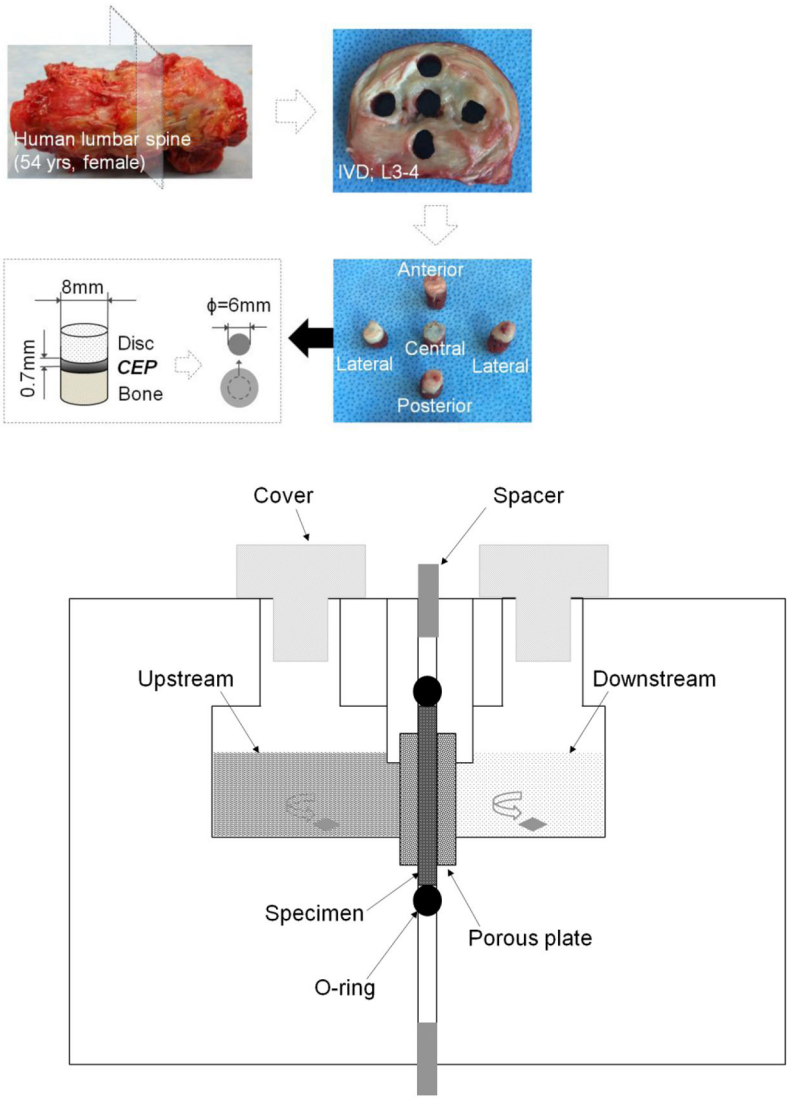

Figure 1.

(A) Schematic of specimen preparation. Human VB/CEP/Disc tissue plugs were harvested from various regions of the disc motion segment (VB: vertebral body). Disc-shape human CEP specimens were prepared using a microtome and corneal trephine for diffusion and biochemical measurements. (B) Schematic of diffusion cell for glucose/lactate diffusivity measurements.

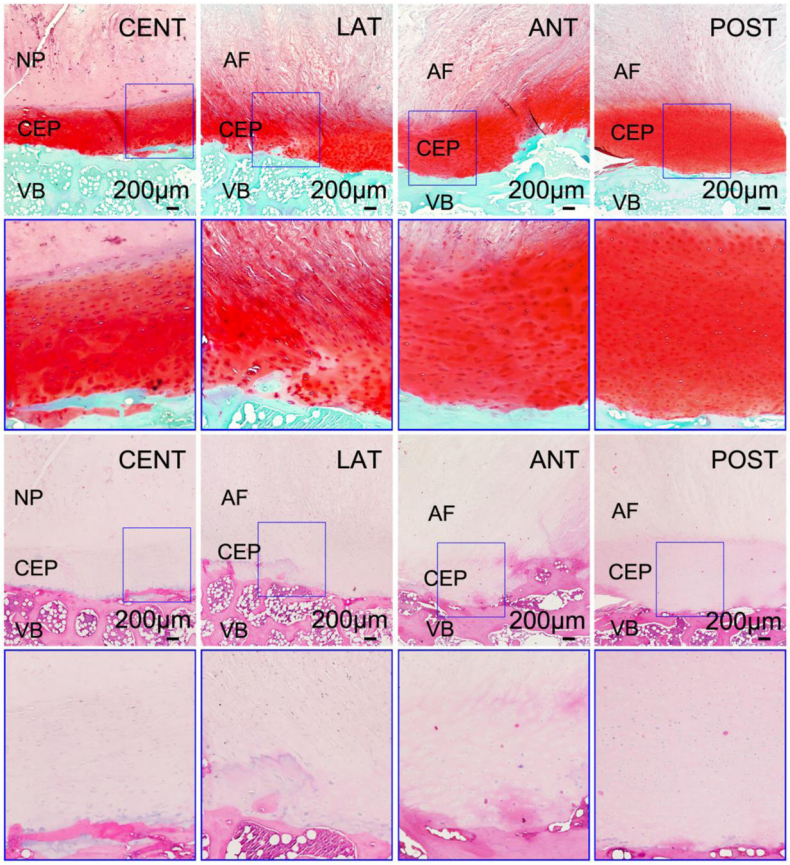

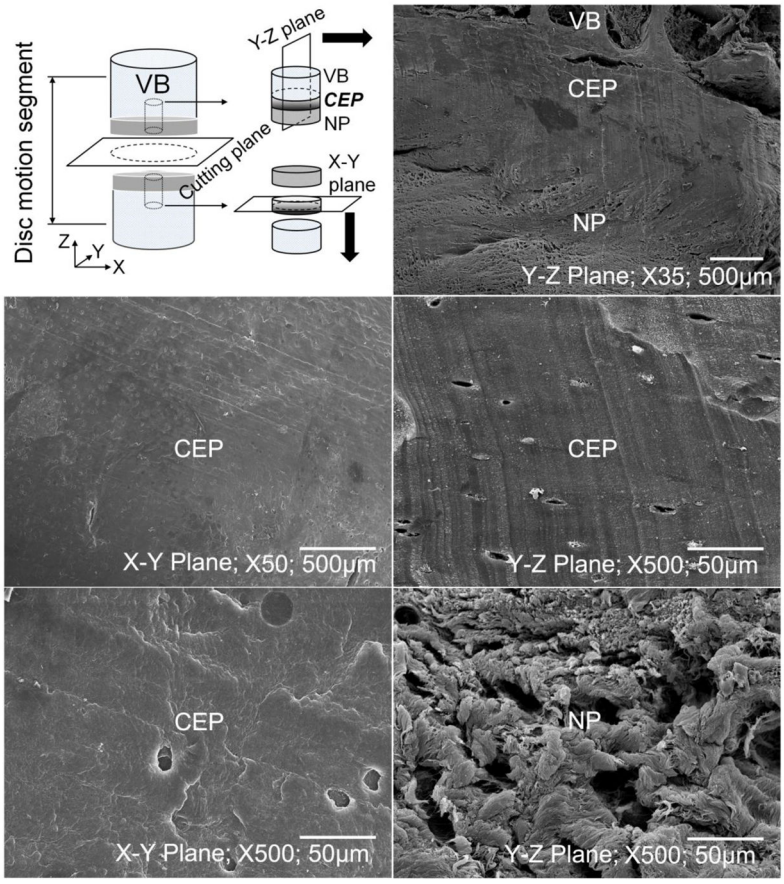

Figure 2.

(A) Histological images for the sandwich structure between the human VB, CEP, and disc tissue (NP or AF) at superior surface of the disc motion segment under 4x and 10x magnifications (10x images with blue outlines were enlarged from the corresponding marked areas in 4x images). The two rows of images on the top were from Safranin-O slices, while the two rows on the bottom were from H&E slices (CENT-Central; LAT-Lateral; ANT-Anterior; POST-Posterior). (B) SEM images for CEP and disc tissue at central region under 35x, 50x, and 500x magnifications.

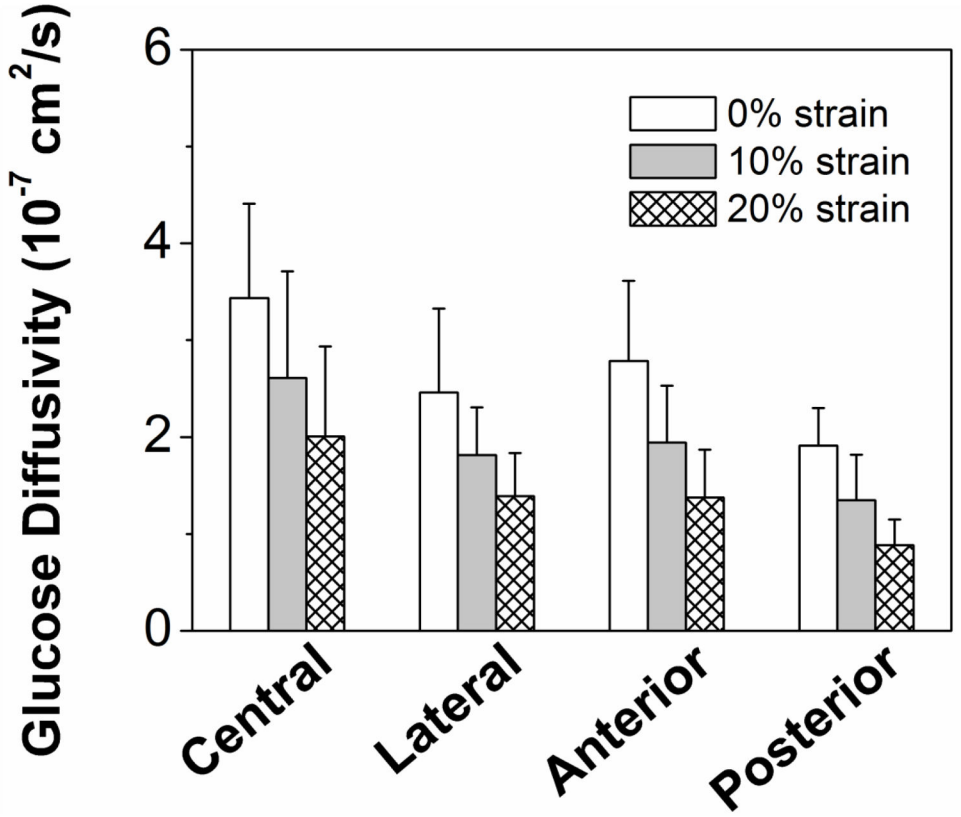

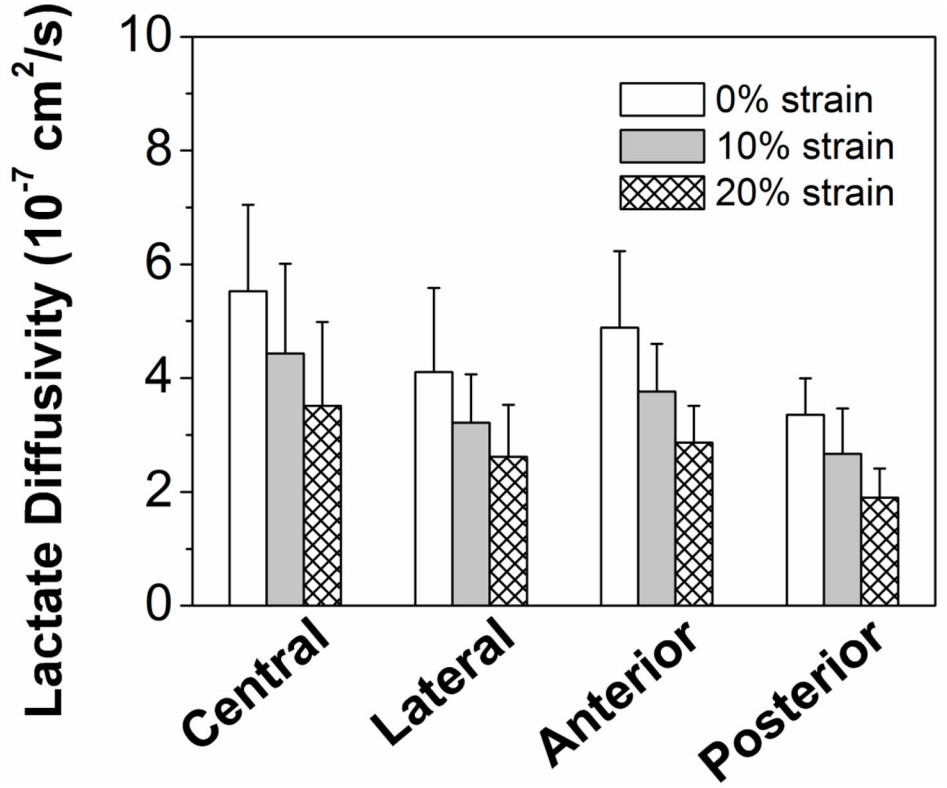

Figure 3.
Effect of compressive strains on the regional distribution of (A) glucose diffusivity and (B) lactate diffusivity of human CEP. (Sample size n=6)

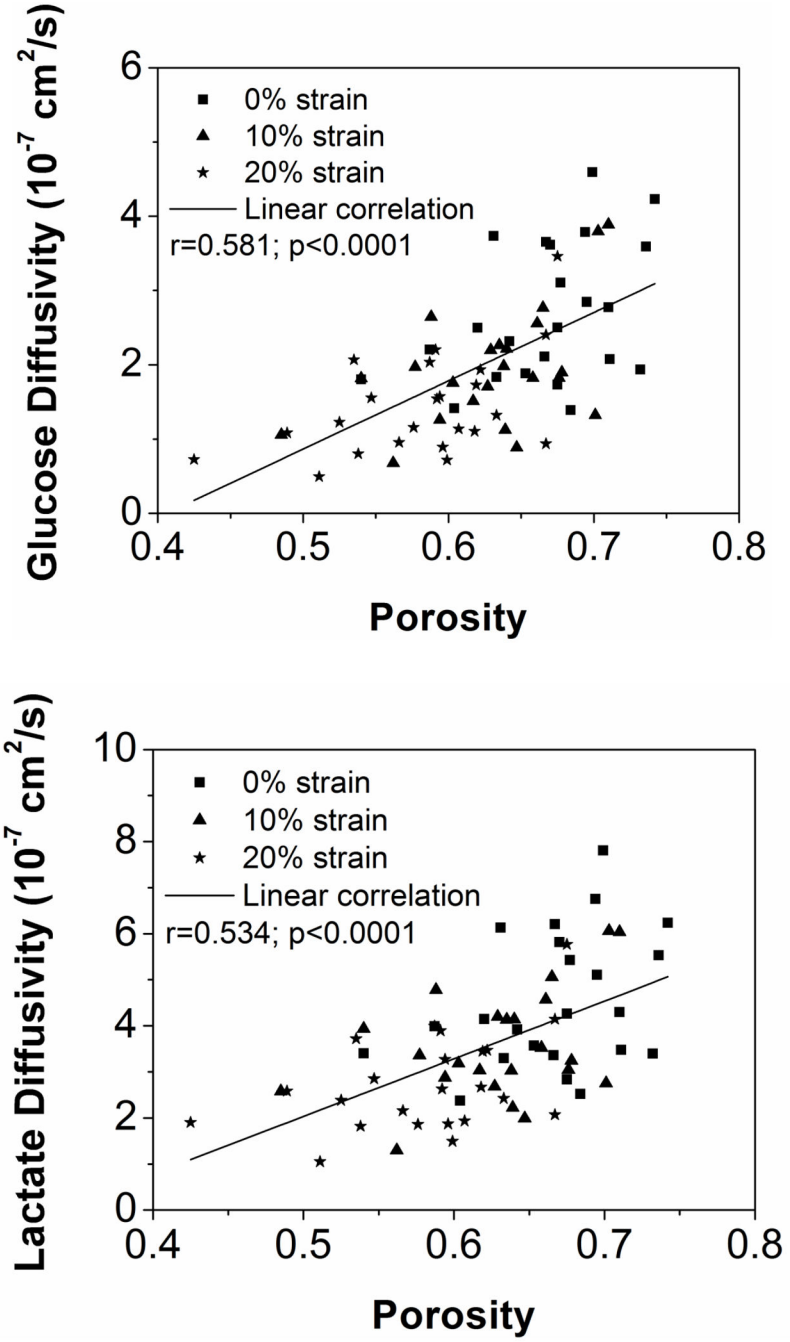

Figure 4.
Correlation between tissue porosity and (A) the glucose diffusivity and (B) the lactate diffusivity. (Sample size n=74)

Table 1

Porosity (Φ^w) at 0% strain and GAG content (mean ± standard deviation) of human CEP in four disc regions.

	Central (n=6)	Lateral (n=6)	Anterior (n=6)	Posterior (n=6)	Average
Φ^w	0.706±0.030	0.680±0.016	0.632±0.061	0.648±0.050	0.667±0.049
GAG *(μg/mg dry tissue)*	109.49±6.99	72.65±16.50	89.18±13.67	84.08±6.34	90.08±17.77

Table 2

Glucose and lactate diffusivities (mean ± standard deviation) in human CEP and other cartilaginous tissues. (CEP: cartilage endplate; AF: annulus fibrosus; AC: articular cartilage)

Species	$D_{Glucose}$ 10^{-7} cm^2/s	$D_{Lactate}$ 10^{-7} cm^2/s	Source
Human CEP	**3.44±0.97-Central** **2.46±0.86-Lateral** **2.78±0.83-Anterior** **1.91±0.39-Posterior**	**5.52±1.52-Central** **4.11±1.48-Lateral** **4.88±1.34-Anterior** **3.36±0.64-Posteror**	**Present study (0% strain)**
Human CEP	5.8±2.1-Central 1.8±0.3-Peripheral	----	(Maroudas, et al., 1975)
Human AF	17±1.5 7.56±0.75	----	(Maroudas, et al., 1975) (Jackson, et al., 2012)
Bovine AF	13.8±0.15	----	(Jackson, et al., 2008)
Human AC	13.5–14.6	----	(Maroudas, 1970)